

**PbSe nanocrystals remain intrinsic after surface adsorption of hydrazine**

Alex Kutana and Steven C. Erwin

*Center for Computational Materials Science, Naval Research Laboratory, Washington, DC 20375-5000, USA*

(Received 20 December 2010; revised manuscript received 21 March 2011; published 15 June 2011)

Recent experiments have shown a dramatic increase in the conductivity of PbSe nanocrystalline films after hydrazine treatment, suggesting that hydrazine may create free carriers in PbSe nanocrystals. Here, we study the effect of hydrazine adsorption on the electronic structure of PbSe nanocrystals using density functional theory. The physisorption of the intact hydrazine molecule and its dissociative chemisorption on different surfaces of PbSe are considered. Despite experimental indications of the *n*-type doping by hydrazine in PbSe, no theoretical evidence of the effect is found. Instead, PbSe is predicted to remain an intrinsic semiconductor after surface doping by hydrazine, and become a *p*-type semiconductor after doping by the hydrazine fragments. We attribute the discrepancy between experiment and theory to indirect effects, such as self-doping by excess surface atoms due to selective surface etching.

DOI: [10.1103/PhysRevB.83.235419](https://doi.org/10.1103/PhysRevB.83.235419)

PACS number(s): 73.20.At, 73.20.Hb, 73.22.-f

**I. INTRODUCTION**

Future technologies based on semiconductor nanocrystals will depend on our ability to control the electronic charge in the material.<sup>1</sup> The charge in bulk semiconductors is normally determined by impurities introduced during growth. In nanocrystals this strategy has been much less successful, and hence the factors that control impurity doping at the nanoscale remain unclear.<sup>2,3</sup> One possible alternative to impurity doping is *surface charge-transfer doping*: the transfer of electrons or holes into a nanocrystal from a molecule bound to its surface. Surface doping may be a viable procedure in colloidal nanocrystals due to the ease with which surfactant molecules are adsorbed during growth. Experimentally, it is well known that surfactants influence the electronic,<sup>4-7</sup> optical,<sup>5,8,9</sup> and chemical<sup>10,11</sup> properties of nanocrystals, as well as their geometric structure.<sup>12-14</sup> For example, treating the surface of PbSe colloidal nanocrystals with hydrazine surfactants<sup>4-9,15-17</sup> dramatically increases the conductivity<sup>6,7,15,17</sup> and photoconductivity<sup>4</sup> of PbSe nanocrystalline films. The origin of this increase has not been established. Two possible mechanisms have been proposed.<sup>5,6,17</sup> First, the intrinsic conductivity of the individual nanocrystals could increase due to carrier doping by hydrazine molecules adsorbed on the surface. Second, the conductivity of the nanocrystalline film could improve as a result of the increased tunneling rate due to the reduced spacing between nanocrystals. This spacing reduction is a result of the displacement of bulky oleic acid from the surface by hydrazine, leading to a narrower tunneling barrier and better conductivity.

In this work, we use first-principles theoretical methods to examine critically the first of these proposed mechanisms. Specifically, we perform electronic structure calculations for hydrazine adsorbed on PbSe nanocrystals to identify the resulting changes in their intrinsic conductivity. We find no evidence of *n*-type doping by hydrazine in PbSe. Instead, the electronic structure of PbSe nanocrystals covered with hydrazine remains intrinsic, whereas adsorption of NH<sub>2</sub> fragments leads to *p*-doping for all surface orientations considered in this work.

**II. METHOD**

In our calculations, the surface facets of PbSe nanocrystals were modeled as planar, infinite surfaces. This approximation reduces computational cost and facilitates the interpretation of the band structure. We expect the model to be valid for PbSe nanocrystals in their typical size range (>5 nm), where their behavior with respect to adsorption and doping is anticipated to be bulklike. To represent the facets on PbSe nanocrystals we used surfaces with crystallographic orientations of (100), (110), and (111). These three orientations are sufficient because they are the ones most often encountered in colloidal PbSe nanocrystals. Indeed, high-resolution transmission electron microscopy (HRTEM) reveals that growing PbSe nanocrystals have simple, regular shapes: octahedron, truncated octahedron, cuboctahedron, truncated cube, and cube. All of these are bounded solely by the (100) and (111) surfaces.<sup>6,11,18</sup> Other HRTEM observations show the occasional presence of (110) surfaces.<sup>19</sup> These shapes occur for a wide variety of growth conditions,<sup>14,20,21</sup> confirming the stability of these three low-index planar facets in PbSe. Nonplanar features such as terraces, kinks, and steps are also possible, of course, but for each of these structures the local atomic environment around a single atom is equivalent to one of the three low-index planar surfaces, as discussed in Ref. 3. For molecules such as hydrazine this local equivalence is broken, so that adsorption near defects must be studied separately; for simplicity we do not consider defects in this work. Bulk-terminated surfaces were used for the (100) and (110) orientations because they are both stable when unreconstructed. For the (111) orientation the “octupolar” rocksalt reconstruction<sup>19,22</sup> was used, as has been done elsewhere.<sup>2</sup> The most favorable location of the adsorbate on the surface was determined by carrying out geometry optimizations beginning from a number (~4) of symmetric sites within the surface unit cell.

Adsorption energies and geometries were determined using density-functional theory (DFT) with two exchange-correlation functionals: Perdew-Burke-Ernzerhof (PBE, Ref. 23), and the van der Waals density functional (vdW-DF, Ref. 24). The PBE functional employs a semilocal generalized

gradient approximation (GGA), whereas the vdW-DF functional augments the GGA correlation energy with a nonlocal term representing van der Waals interactions. The performance of vdW-DF on noncovalent molecular complexes<sup>25</sup> was previously found to be superior to that of plain GGA. In both approaches, we used the projector-augmented wave method<sup>26</sup> as implemented in GPAW.<sup>27</sup> In contrast with most periodic density-functional theory (DFT) methods, GPAW represents the Kohn-Sham orbitals on a real-space grid instead of through a plane-wave basis. Here a grid interval of 0.18 Å was used along each coordinate. The nanocrystal surface facets were modeled as planar, infinite surfaces and represented by slabs of 8–16 atomic layers. The surface Brillouin zone was sampled on  $2 \times 2$  (for geometry optimization) and  $16 \times 16$  (for band-structure calculations) Monkhorst-Pack grids. Spin-unpolarized calculations were carried out for isolated molecules and extended structures. The reference energy for the eigenvalues was chosen to be the value of the local (Hartree) potential away from the surface. Care has been taken to ensure that the vacuum region is large enough for the Hartree potential to be constant in that region, and that the obtained eigenvalues are insensitive to the vacuum size. The minimization procedure was considered converged when the maximum component of the force acting on any atom was smaller than 0.05 eV/Å. Both  $1 \times 1$  and  $2 \times 2$  surface supercells were tested and yielded nearly identical results. The PbSe surface was kept frozen during minimization. This assumption is justified for the cases of weak interactions considered here; surface relaxations are expected to be small in such cases.

### III. RESULTS

#### A. Physisorption of hydrazine

Initially, the adsorption of intact hydrazine molecules was considered. The lowest-energy equilibrium structures for

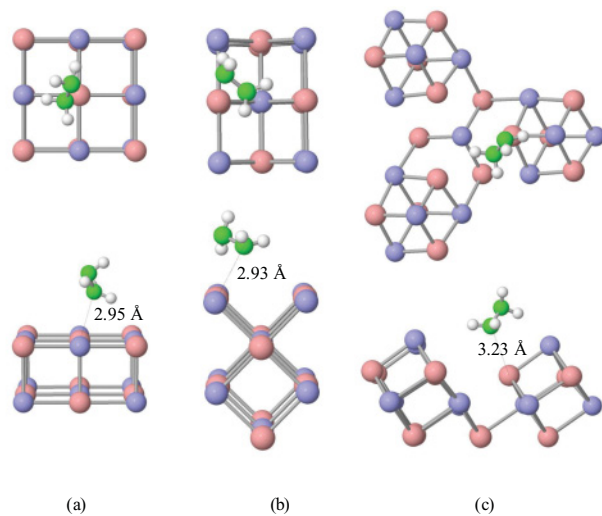


FIG. 1. (Color online) Top and side views of hydrazine ( $\text{N}_2\text{H}_4$ ) adsorbed on a PbSe surface with crystallographic orientation (100), (110), and (111) [panels (a), (b), and (c)]. Only the lowest-energy adsorbed configurations, in their equilibrium structure, are shown. Lead atoms are pink (lighter circles), selenium atoms are blue (darker circles), nitrogen atoms are green, and hydrogen atoms are white.

hydrazine physisorption are shown in Fig. 1. Despite the morphological differences among the three PbSe surfaces, the most favorable adsorbate configurations share several common features: (1) The preferred adsorption site of the hydrazine molecule is near a surface lead atom. (2) The closest distance from a nitrogen atom to a surface lead atom is approximately 3 Å in both PBE and vdW-DF approximations, which is characteristic of noncovalent interactions. (3) The hydrazine adopts an orientation in which two hydrogen atoms on the lower nitrogen atom face away from the surface lead atom. Hydrazine is a Lewis base in which lone-pair electron donors reside on each of the nitrogen atoms; the electron pair on the lower nitrogen could, in principle, be donated to the surface. In this scenario the nearest surface lead atom would act as the acceptor. This transfer of electrons, if it occurs, would change the electronic state of the nanocrystal from intrinsic to  $n$ -type.

Figure 2 shows the calculated energy levels of an isolated hydrazine molecule, and the band gaps and Fermi levels for the (100), (110), and (111) surfaces before and after hydrazine adsorption. Before adsorption occurs, the highest occupied levels (the lone pairs of electrons) on the hydrazine molecule lie at roughly  $-6$  eV, well in the valence band of all three surfaces. After adsorption, this alignment remains qualitatively unchanged. As a result, the PbSe does not have any empty levels to accept electrons from the lone pair and therefore little or no charge transfer can occur. For this reason, the Fermi level remains in the middle of the band gap on all three surfaces throughout the range of hydrazine coverage considered here, 0.25–0.50 monolayer. Although the adsorption of hydrazine causes the Fermi level on all three surfaces to shift upward as a dipole layer is formed on the surface, the band gap is essentially unaffected.

Earlier explanations of the increased conductivity of PbSe nanocrystalline films treated with hydrazine<sup>5,6,17</sup> were based on the fact that  $\text{N}_2\text{H}_4$  is a strong Lewis base and therefore might be expected to function as an electron donor. However, the lead atom in the host PbSe crystal is also an electron donor and will compete with other donors. The outcome will depend on the relative electronegativity and hardness of the competing donors. We find that the intact hydrazine molecule and the PbSe surface do not form a charge-transfer complex. Specifically, our analysis of Bader charges<sup>28,29</sup> shows that no significant electron transfer results from adsorption. For example, the Bader charge of a Pb atom is  $+0.85$  in the bulk and  $+0.88$  on the clean (100) surface. After hydrazine adsorption, the charge on the Pb atom closest to the adsorbate shows a negligible increase of less than 0.01. Likewise, the charge on the Se atom is  $-0.85$  on the clean surface and is reduced by less than 0.02 upon hydrazine adsorption. Thus, the overall charge transfer from the adsorbate to the surface is only on the order of 0.01 electron. This is insufficient to explain the experimentally observed increase in conductivity.

#### B. Dissociative chemisorption of hydrazine

We also considered the possibility that hydrazine might adsorb on PbSe dissociatively, by splitting into two  $\text{NH}_2$  fragments. Dissociative chemisorption is most often encountered in heterogeneous catalysis. While most known heterogeneous catalysts are elemental metals, it may be possible that the

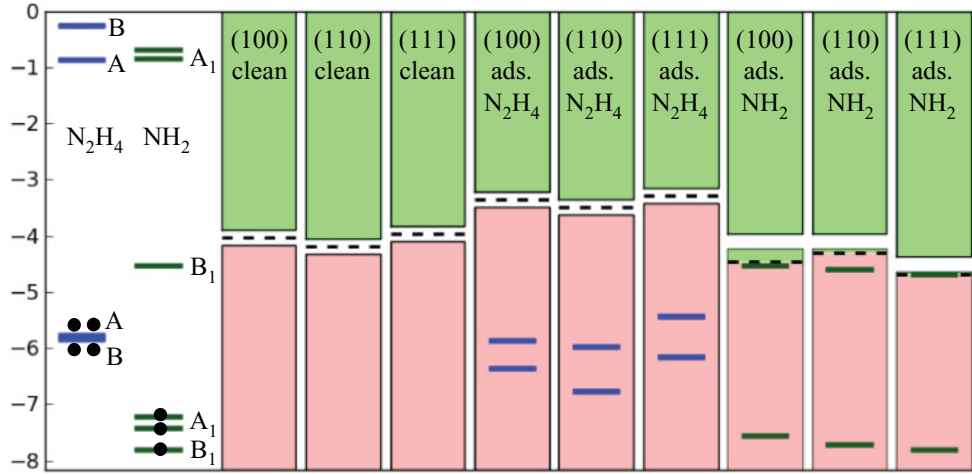


FIG. 2. (Color online) Theoretical electronic structures of the isolated hydrazine molecule and isolated  $\text{NH}_2$  fragment (left), and the PbSe (100), (110), and (111) surfaces, in both the clean and adsorbed states (right). Occupancies and Mulliken symbols are shown for the electronic levels of hydrazine and  $\text{NH}_2$ . For clean and hydrazine-adsorbed surfaces, the Fermi level falls inside the projected band gap, showing that hydrazine adsorption does not create free electrons or holes on these surfaces. On  $\text{NH}_2$ -adsorbed surfaces, free holes are created by the electron transfer from the valence band to an empty  $B_1$  state on the  $\text{NH}_2$  fragment. For the adsorbed surfaces, the occupied molecular-like states (blue lines, hydrazine; green lines,  $\text{NH}_2$ ) are shown. These remain energetically close to the corresponding states of the isolated molecule.

surface of lead selenide is capable of splitting the N-N bond in hydrazine. The likelihood of this process depends, in part, on the adsorbate binding energy of a neutral  $\text{NH}_2$  fragment compared with that of an intact  $\text{N}_2\text{H}_4$  molecule. Table I shows the theoretical adsorption binding energies of intact  $\text{N}_2\text{H}_4$  molecules and  $\text{NH}_2$  fragments, defined with respect to the intact molecule at infinity:

$$E_b = -[E(\text{PbSe} + \text{NH}_2) - E(\text{PbSe}) - E(\text{N}_2\text{H}_4)]/2.$$

The adsorption energies were calculated using the PBE and vdW-DF density functionals. Both functionals show that the interactions of the intact hydrazine molecules with the surface are attractive, whereas the stability of the  $\text{NH}_2$  fragments depends on the surface type. From the comparison of the values given by the two functionals, the contribution of van der Waals interactions into the total binding energy may be assessed. It follows that van der Waals interactions comprise about 20% of the binding energy of hydrazine. They also contribute toward the stabilization of the adsorption of  $\text{NH}_2$  fragments, although the dissociation of hydrazine remains energetically unfavorable on the (100) or (111) surfaces with

TABLE I. Theoretical binding energies,  $E_b$ , of the hydrazine molecule,  $\text{N}_2\text{H}_4$ , and of a hydrazine fragment,  $\text{NH}_2$ , on three low-index facets of PbSe (in eV). The binding energies are defined with respect to the infinitely separated intact  $\text{N}_2\text{H}_4$  molecule and the clean PbSe surface. Larger positive binding energies indicate more stable configurations.

PbSe facet	$E_b(\text{N}_2\text{H}_4)$		$E_b(\text{NH}_2)$	
	PBE	vdW-DF	PBE	vdW-DF
(100)	0.34	0.46	-0.82	-0.66
(110)	0.45	0.54	0.13	0.23
(111)	0.26	0.35	-0.67	-0.51

or without van der Waals interactions. Comparison of the binding energies for intact molecules and fragments suggests that hydrazine *may* adsorb dissociatively on the (110) surface but will not do so on the (100) and (111) surfaces. Specifically, dissociative adsorption on the (110) surface shows a stable configuration with a positive binding energy of 0.23 eV. The energy of this configuration is only slightly higher (by 0.04 eV per  $\text{NH}_2$  fragment) than for the intact hydrazine molecule. Hence it is possible that the molecule coexists in both intact and dissociated states on the (110) surface. In contrast, on the (100) and (111) surfaces the dissociated adsorbed state is unstable with respect to both the intact adsorbed state and the intact desorbed state, and hence dissociative adsorption on these facets is unlikely.

Setting aside for a moment the plausibility of dissociative hydrazine adsorption, we find that the adsorbed  $\text{NH}_2$  fragments lead to *p*-doping on all three surfaces examined. The key difference with the adsorption of hydrazine is the presence of an empty  $\text{NH}_2$  orbital that is created after the homolytic splitting of the hydrazine N-N bond. As seen in Fig. 2, the energy of this orbital lies slightly below the maximum of the valence band of PbSe, making the transfer of an electron from the surface to the fragment energetically favorable. Bader charge analysis confirms the presence of electron transfer after the  $\text{NH}_2$  adsorption, with the surface Pb atom being the main electron donor and the N atom being the electron acceptor. It follows that 0.38 electron is transferred to the N atom on PbSe(100), 0.47 electron on PbSe(110), and 0.41 electron on PbSe(111) surface. This electron transfer leads to the shift of the Fermi level into the semiconductor valence band, as shown in Fig. 2. Now the doped surface has empty states above the Fermi level, as expected for a *p*-type semiconductor. The atom-projected density of state (DOS) analysis shows the presence of a filled state on the N atom that is located below the Fermi level, as shown in Fig. 2, confirming the filling of an empty  $\text{NH}_2$  orbital by the electron from the surface.

#### IV. DISCUSSION AND CONCLUSIONS

The theoretical evidence presented above suggests that the adsorption of intact hydrazine does not affect the conductivity of PbSe significantly, whereas the  $\text{NH}_2$  fragment may act as a  $p$ -dopant, provided that the dissociation of hydrazine on the surface is thermodynamically feasible. In view of our findings, the question remains as to why the experimental evidence points to the  $n$ -type conductivity<sup>5,6,17</sup> in PbSe nanocrystals treated with hydrazine. We propose that in addition to direct creation of carriers by hydrazine adsorption, they may also be created indirectly by various means. For instance, it is plausible that the adsorption of hydrazine displaces the oleic acid molecules that normally passivate PbSe nanocrystals. Oleic acid by itself is an electron acceptor and thus its removal would allow other sources of electrons (e.g., excess surface lead atoms<sup>12</sup>) to render the nanocrystal  $n$ -type. Other, more direct, mechanisms not considered in this work may also be at play: for example, the insertion of hydrazine molecules or fragments into the crystalline lattice (a kind of bulk doping), or selective etching of the surface atoms, may lead to either  $n$ - or  $p$ -type doping. The reversal of the conductivity type due to the creation of trapped surface states by etching has been previously reported in CdSe quantum dots<sup>30</sup> and  $\text{TiO}_2$  nanocrystals.<sup>31</sup> There, the conductivity type could be

switched from  $n$ - to  $p$ -type after mild etching with HCl. The underlying mechanism behind switching is the trapping of charge carriers in surface states leading to change in the type of the majority carrier. In PbSe nanocrystals, etching of the surface by hydrazine could similarly create trapped states. This mechanism of conductivity switching through the creation of trapped states would provide an explanation of the reported experimental observations in PbSe nanocrystals without the need to invoke electron donation by hydrazine.

In conclusion, we examined the possibility of doping of PbSe nanocrystals by surface adsorption of hydrazine. Despite earlier experimental reports of  $n$ -type doping, we find that the adsorption of hydrazine on the surfaces of PbSe nanocrystals has no direct effect on their intrinsic conductivity, whereas the adsorbed  $\text{NH}_2$  fragment actually acts as a  $p$ -type dopant. We attribute the experimental observations of  $n$ -doping by hydrazine to indirect effects such as trapped states created by etching.

#### ACKNOWLEDGMENT

This work was performed under the ASEE program at the Naval Research Laboratory. Computations were performed at the DoD Shared Resource Center at ARSC.

- <sup>1</sup>D. J. Norris, A. L. Efros, and S. C. Erwin, *Science* **319**, 1776 (2008).
- <sup>2</sup>S. C. Erwin, L. J. Zu, M. I. Haftel, A. L. Efros, T. A. Kennedy, and D. J. Norris, *Nature (London)* **436**, 91 (2005).
- <sup>3</sup>S. C. Erwin, *Phys. Rev. B* **81**, 235433 (2010).
- <sup>4</sup>J. E. Murphy, M. C. Beard, and A. J. Nozik, *J. Phys. Chem. B* **110**, 25455 (2006).
- <sup>5</sup>M. Law, J. M. Luther, O. Song, B. K. Hughes, C. L. Perkins, and A. J. Nozik, *J. Am. Chem. Soc.* **130**, 5974 (2008).
- <sup>6</sup>D. V. Talapin and C. B. Murray, *Science* **310**, 86 (2005).
- <sup>7</sup>K. J. Williams, W. A. Tisdale, K. S. Leschkes, G. Haugstad, D. J. Norris, E. S. Aydil, and X. Y. Zhu, *ACS Nano* **3**, 1532 (2009).
- <sup>8</sup>J. M. Luther, M. C. Beard, Q. Song, M. Law, R. J. Ellingson, and A. J. Nozik, *Nano Lett.* **7**, 1779 (2007).
- <sup>9</sup>B. A. Timp and X. Y. Zhu, *Surf. Sci.* **604**, 1335 (2010).
- <sup>10</sup>C. Schliehe, B. H. Juarez, M. Pelletier, S. Jander, D. Greshnykh, M. Nagel, A. Meyer, S. Foerster, A. Kornowski, C. Klinke, and H. Weller, *Science* **329**, 550 (2010).
- <sup>11</sup>K. S. Cho, D. V. Talapin, W. Gaschler, and C. B. Murray, *J. Am. Chem. Soc.* **127**, 7140 (2005).
- <sup>12</sup>I. Moreels, B. Fritzing, J. C. Martins, and Z. Hens, *J. Am. Chem. Soc.* **130**, 15081 (2008).
- <sup>13</sup>W. K. Koh, A. C. Bartnik, F. W. Wise, and C. B. Murray, *J. Am. Chem. Soc.* **132**, 3909 (2010).
- <sup>14</sup>Y. J. Na, H. S. Kim, and J. Park, *J. Phys. Chem. C* **112**, 11218 (2008).
- <sup>15</sup>S. J. Kim, W. J. Kim, Y. Sahoo, A. N. Cartwright, and P. N. Prasad, *Appl. Phys. Lett.* **92**, 031107 (2008).
- <sup>16</sup>S. J. Kim, W. J. Kim, A. N. Cartwright, and P. N. Prasad, *Appl. Phys. Lett.* **92**, 191107 (2008).
- <sup>17</sup>D. V. Talapin, C. T. Black, C. R. Kagan, E. V. Shevchenko, A. Afzali, and C. B. Murray, *J. Phys. Chem. C* **111**, 13244 (2007).
- <sup>18</sup>D. V. Talapin, H. Yu, E. V. Shevchenko, A. Lobo, and C. B. Murray, *J. Phys. Chem. C* **111**, 14049 (2007).
- <sup>19</sup>C. M. Fang, M. A. van Huis, D. Vanmaekelbergh, and H. W. Zandbergen, *ACS Nano* **4**, 211 (2010).
- <sup>20</sup>W. G. Lu, J. Y. Fang, Y. Ding, and Z. L. Wang, *J. Phys. Chem. B* **109**, 19219 (2005).
- <sup>21</sup>K. Ahmad, M. Afzaal, P. O'Brien, G. X. Hua, and J. D. Woollins, *Chem. Mater.* **22**, 4619 (2010).
- <sup>22</sup>A. Barbier, C. Mocuta, H. Kuhlbeck, K. F. Peters, B. Richter, and G. Renaud, *Phys. Rev. Lett.* **84**, 2897 (2000).
- <sup>23</sup>J. P. Perdew, K. Burke, and M. Ernzerhof, *Phys. Rev. Lett.* **77**, 3865 (1996).
- <sup>24</sup>M. Dion, H. Rydberg, E. Schroder, D. C. Langreth, and B. I. Lundqvist, *Phys. Rev. Lett.* **92**, 246401 (2004).
- <sup>25</sup>A. Tkatchenko, L. Romaner, O. T. Hofmann, E. Zojer, C. Ambrosch-Draxl, and M. Scheffler, *MRS Bull.* **35**, 435 (2010).
- <sup>26</sup>P. E. Blochl, *Phys. Rev. B* **50**, 17953 (1994).
- <sup>27</sup>J. Enkovaara, C. Rostgaard, J. J. Mortensen, J. Chen, M. Dulak, L. Ferrighi, J. Gavnholt, C. Glinsvad, V. Haikola, H. A. Hansen, H. H. Kristoffersen, M. Kuisma, A. H. Larsen, L. Lehtovaara, M. Ljungberg, O. Lopez-Acevedo, P. G. Moses, J. Ojanen, T. Olsen, V. Petzold, N. A. Romero, J. Stausholm-Moller, M. Strange, G. A. Tritsarlis, M. Vanin, M. Walter, B. Hammer, H. Hakkinen, G. K. H. Madsen, R. M. Nieminen, J. Norskov, M. Puska, T. T. Rantala, J. Schiøtz, K. S. Thygesen, and K. W. Jacobsen, *J. Phys.: Condens. Matter* **22**, 253202 (2010).
- <sup>28</sup>R. F. W. Bader, *Atoms in Molecules: A Quantum Theory* (Oxford University Press, New York, 1990).
- <sup>29</sup>W. Tang, E. Sanville, and G. Henkelman, *J. Phys. Condens. Matter* **21**, 084204 (2009).
- <sup>30</sup>L. Kronik, N. Ashkenasy, M. Leibovitch, E. Fefer, Y. Shapira, S. Gorer, and G. Hodes, *J. Electrochem. Soc.* **145**, 1748 (1998).
- <sup>31</sup>D. S. Warren, Y. Shapira, H. Kisch, and A. J. McQuillan, *J. Phys. Chem. C* **111**, 14286 (2007).